

Black Phosphorus based One-dimensional Photonic Crystals and Microcavities

Ilka Kriegel¹, Stefano Toffanin², Francesco Scotognella^{3,4*}

¹Department of Nanochemistry, Istituto Italiano di Tecnologia (IIT), via Morego, 30, 16163 Genova, Italy

²Istituto per lo Studio dei Materiali Nanostrutturati, Consiglio Nazionale delle Ricerche (CNR-ISMN), via Gobetti 101, 40129 Bologna, Italy

³Dipartimento di Fisica, Istituto di Fotonica e Nanotecnologie CNR, Politecnico di Milano, Piazza Leonardo da Vinci 32, 20133 Milano, Italy

⁴Center for Nano Science and Technology@PoliMi, Istituto Italiano di Tecnologia, Via Giovanni Pascoli, 70/3, 20133, Milan, Italy

* Corresponding author at: Dipartimento di Fisica, Politecnico di Milano, Piazza Leonardo da Vinci 32, 20133 Milano, Italy. E-mail address: francesco.scotognella@polimi.it

Abstract

The latest achievements in the fabrication of black phosphorus thin layers, towards the technological breakthrough of a phosphorene atomically thin layer, are paving the way for their employment in electronics, optics, and optoelectronics. In this work, we have simulated the optical properties of one-dimensional photonic structures, i.e. photonic crystals and microcavities, in which few-layer black phosphorus is one of the components. The insertion of the 5 nm black phosphorous layers leads to a photonic band gap in the photonic crystals and a cavity mode in the microcavity interesting for light manipulation and emission enhancement.

Keywords: black phosphorus; optical properties; photonic crystal.

Introduction

In the last years a lot of effort has been spent by many scientists in the materials science and solid state physics research community to obtain novel layered semiconducting materials, to tailor their properties and to integrate them as building blocks into electronic and optoelectronic devices [1,2]. Black phosphorus is particularly interesting since, in terms of electronic band gap energy, it fills the gap between graphene and metallic dichalcogenides on one side (with gaps from zero to about 0.3 eV) and semiconducting dichalcogenides on the other side (with gaps from 1 eV to 2 eV) [3–5]. In fact, black phosphorus has a band gap of 0.3 eV in the bulk and it is predicted a layer-dependent band gap [6] of up to 2 eV [7–10].

The optical properties of layered black phosphorus are characterized by strong photoluminescence [6,11] and the in-plane anisotropy [12]. In Ref. [12] the authors have measured such in-plane anisotropy by polarized optical microscopy and determined the complex refractive index dispersion in the visible range for the in-plane directions.

With the determination of the complex refractive index dispersion it is possible to design optical devices such as photonic crystals and microcavities, useful for the fabrication of optical filters, electro-optic switches and emitters with a tailored luminescence profile [13–16]. Layered semiconducting materials can be straightforwardly integrated in multilayer structures as one-dimensional (1D) photonic crystals and microcavities [17,18].

In this work, we propose the design of BP based 1D photonic crystals and microcavities. We have considered the in-plane anisotropy measured in Ref. [12] and have simulated with the transfer matrix method the transmission spectrum of the photonic structures. In the 1D photonic crystals, BP is alternated with indium tin oxide, while in the microcavity a trilayer silicon dioxide (SiO₂)/BP/SiO₂ a defect layer between two SiO₂/germanium dioxide (GeO₂)

photonic crystals (usually called distributed Bragg reflectors, DBR). The arising of a photonic band gap in the photonic crystals and a cavity mode in the microcavity envisages the fabrication of BP based photonic structures for sensing and lighting applications.

Methods

We have used the refractive index dispersion of black phosphorus as reported in Ref. [12]. As well described in the reference, we have to consider the in-plane anisotropy, thus a refractive index in the AC direction and in the ZZ direction. In this work we refer to the black phosphorus in the AC direction with acBP, and to the black phosphorus in the ZZ direction with zzBP.

We have used the refractive index dispersion of indium tin oxide as reported in Ref. [19], the refractive index dispersion of silicon dioxide as reported in Ref. [20], and the refractive index dispersion of germanium dioxide as reported in Ref. [21] to simulate the dielectric properties of the respective layers.

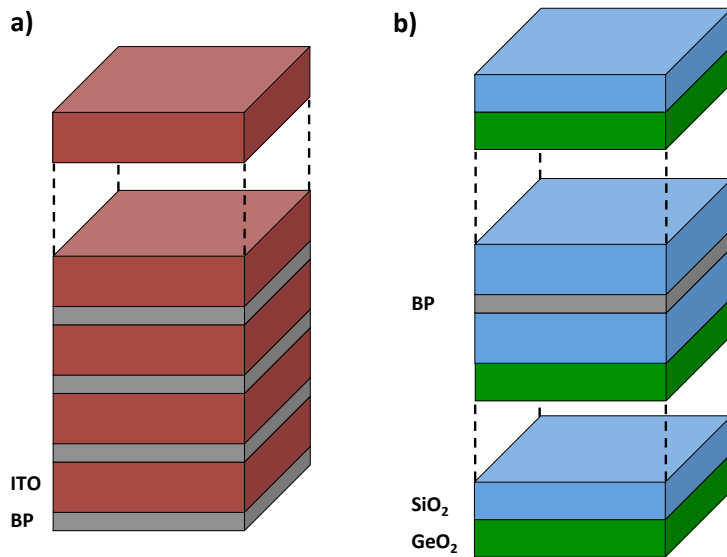


Figure 1. a) sketch of the BP/ITO 1D photonic crystal; b) sketch of the $(\text{GeO}_2/\text{SiO}_2)_{14.5}\text{SiO}_2/\text{BP}/\text{SiO}_2(\text{GeO}_2/\text{SiO}_2)_{14}$ microcavity.

We have considered a 1D photonic crystal in which acBP or zzBP are alternated with ITO, and a microcavity with a BP defect. The sketches of the 1D photonic crystals and the microcavity are reported in Figure 1. In the photonic crystal the thickness of black phosphorus is 5 nm as given in reference [12], while the thickness of indium tin oxide is 154 nm. The number of ac(zz)BP/ITO bilayers is 27. In the microcavity, the 1D structure is composed by a DBR of 14.5 bilayers of germanium dioxide (thickness of 90 nm) and silicon dioxide (thickness of 90 nm), a 5 nm thick layer sandwiched between two 80 nm thick layers of silicon dioxide, and a DBR of 14 bilayer of germanium dioxide and silicon dioxide. The trilayer $\text{SiO}_2/\text{acBP}/\text{SiO}_2$ acts as defect in the microcavity, as in the case of $\text{SiO}_2/\text{MoS}_2/\text{SiO}_2$ in the work reported in Ref. [17]. For the microcavity we have employed only the AC axis of BP. However, the optical properties of a microcavity embedding zzBP can be simulated in a similar way.

The transmission spectra of the photonic crystals and the microcavity have been simulated with the transfer matrix method [22–25]. We have simulated the transmission spectra in the visible range, in which the complex refractive index of BP has been determined [12].

Results and Discussion

In Figure 2a we show the absorption spectrum of the 27 bilayer acBP/ITO photonic crystal, following the architecture depicted in Figure 1a. We have simulated the transmission spectrum and converted it to absorption ($A = -\log_{10} T$). The red dashed curve indicates the absorption of the acBP/ITO photonic crystal taking into account only the real part of the refractive index of acBP. In this way, the occurrence of the photonic band gap at about 600 nm is clear. The black solid curve relates to the absorption of the same photonic crystal, but in this case the complex refractive index of acBP is taken into account, stressing the fact that in the visible range the imaginary part of the refractive index plays a significant role due to the absorption properties of BP in this wavelength range.

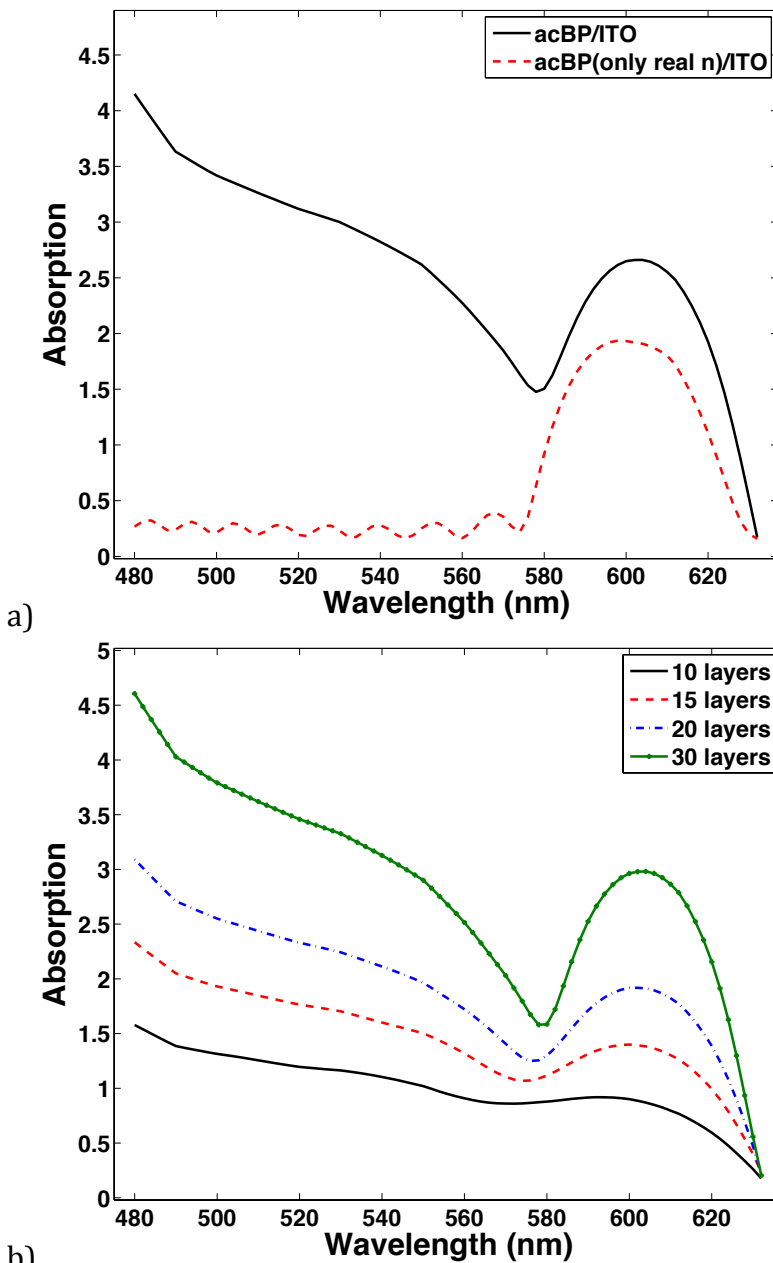
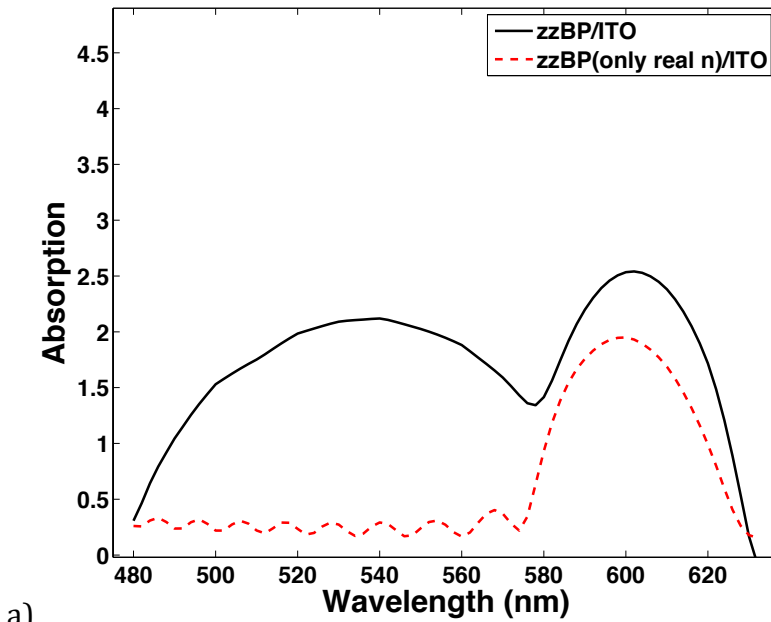


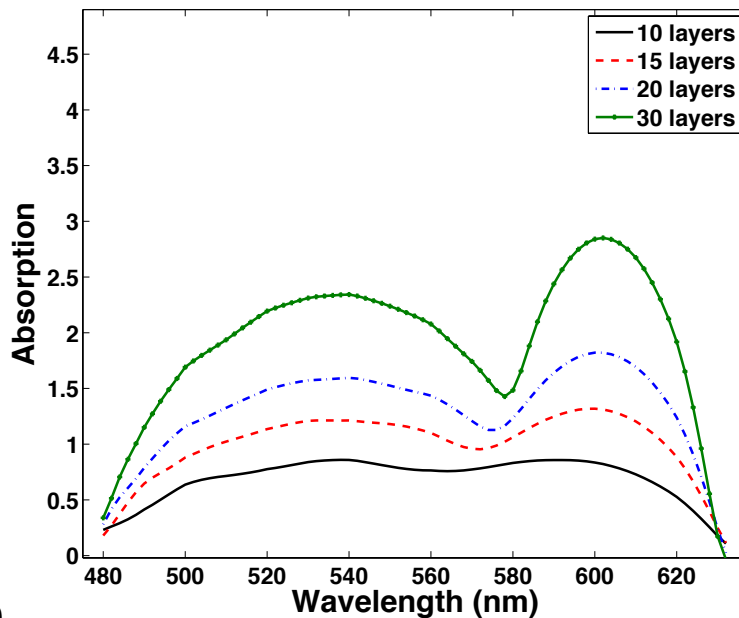
Figure 2. a) Transmission spectrum of 27 bilayer acBP/ITO 1D photonic crystal, where the black solid curve corresponds to the complex refractive index of acBP and the red dashed curve relates only to the real part of the refractive index of acBP; b) transmission spectra of acBP/ITO photonic crystals with different numbers of bilayers.

In Figure 2b we show the absorption spectra of the acBP/ITO photonic crystals for different numbers of acBP/ITO bilayers. The higher the number of alternating layers, the more pronounced the photonic bandgap around 600 nm.

We would like to stress that the alternation of acBP(zzBP) with ITO is very promising for a conductance of charge in the normal direction, due to good charge mobility of both materials. Figure 3a and Figure 3b display the absorption spectra for the zzPB, highlighting that the main difference between the two acBP-based and the zzBP-based photonic crystals is in the absorption in the blue region of the spectra.



a)



b)

Figure 3. a) transmission spectrum of 27 bilayer zzBP/ITO 1D photonic crystal, where the black solid curve corresponds to the complex refractive index of zzBP and the red dashed curve relates only to the real part of the refractive index of zzBP; b) transmission spectra of zzBP/ITO photonic crystals with different numbers of bilayers.

With the $(\text{GeO}_2/\text{SiO}_2)_{14.5}\text{SiO}_2/\text{acBP}/\text{SiO}_2(\text{GeO}_2/\text{SiO}_2)_{14}$ microcavity it is possible to obtain a narrow cavity mode (Figure 4). If we take into account only the real part of the refractive

index of acBP, we observe and high transmissive cavity in the middle of the photonic band gap. Since the BP layer, as experimentally reported in literature [12], is very thin (5 nm), we have embedded the BP layer between two layer of SiO₂. This allows us to have an optical length of the defect layer, i.e. the SiO₂/acBP/SiO₂ layer, comparable to $\lambda/2$.

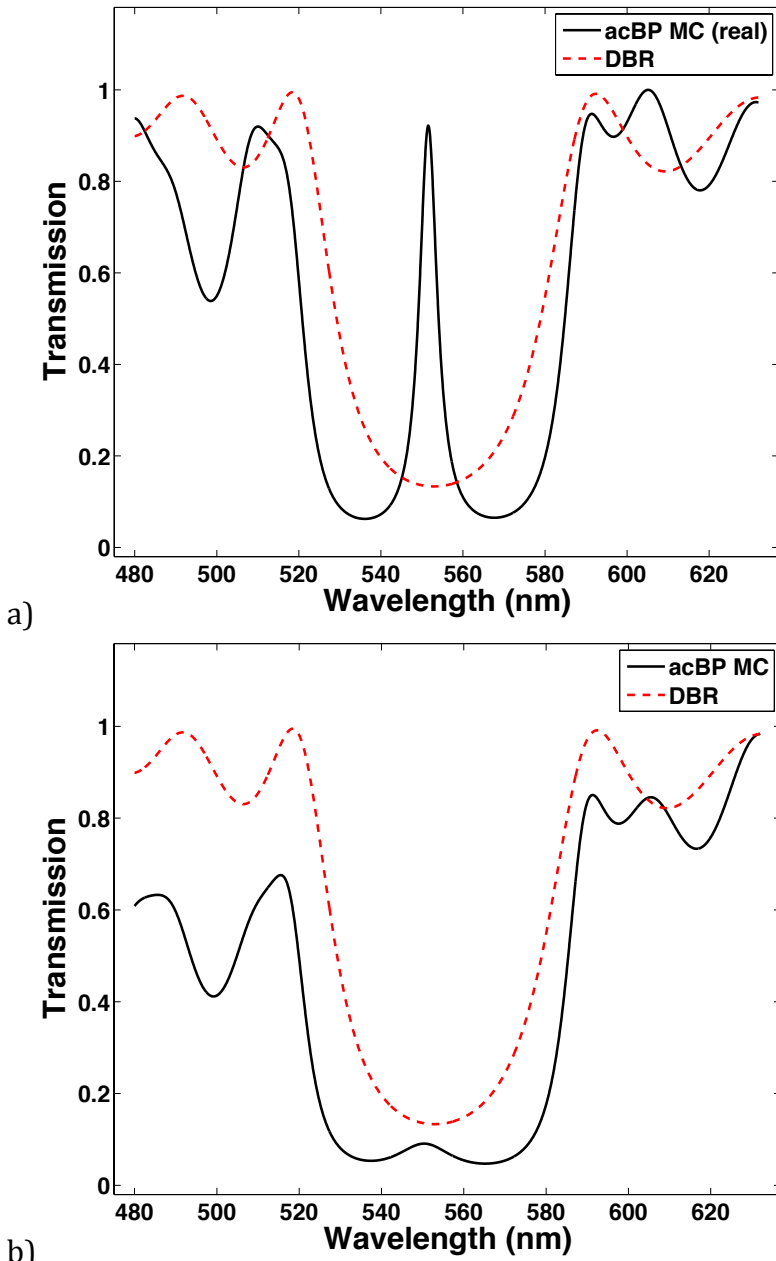


Figure 4. Transmission spectra of: a) a $(\text{GeO}_2/\text{SiO}_2)_{14.5}\text{SiO}_2/\text{acBP}/\text{SiO}_2(\text{GeO}_2/\text{SiO}_2)_{14}$ microcavity where only the real part of the refractive index is taken into account (black solid curve) and the $(\text{GeO}_2/\text{SiO}_2)_{14}$ DBR (red dashed curve); b) the same microcavity with the complex refractive index of BP (black solid curve) and the $(\text{GeO}_2/\text{SiO}_2)_{14}$ DBR (red dashed curve).

In Figure 4b the transmission spectrum takes into account the complex refractive index of acBP. The low transmission in correspondence of the cavity is due to the strong acBP absorption (i.e. imaginary part of the refractive index).

The microcavity could be very interesting for the filtering, and possibly the enhancement, of the luminescence of BP [6,11]. However, to design a proper microcavity for this purpose, the

refractive index dispersion of BP in the photoluminescence range is needed, e.g. in the range between 900 nm to 1600 nm [6].

We want to stress that the realization of the multilayer BP-based photonic systems we have described in the present article is feasible and compatible with the available fabrication protocols usually implemented for exfoliating BP. In particular, oxides other than SiO₂ are demonstrated to form van der Waals junctions at the interface with BP. Consequently, heterostructures comprised by BP and oxides are used in the active region in planar and vertical optoelectronic devices as semiconductor only or insulator/semiconductor systems [26,27]. Typically, the BP flakes are mechanically exfoliated by using scotch tape from single crystal bulk BP and then transferred onto the substrates of interest by means of polydimethylsiloxane (PDMS) elastomer. The possibility to insert BP flakes within a planar microcavity is compatible with these fabrication protocols, as it is demonstrated by the realization of devices with oxide layers deposited on top of BP flakes (i.e. dual-gate or encapsulated top-gate field-effect transistor devices) [28,29]. Moreover, the typical deposition techniques used for fabricating multilayer PhCs such as Pulse Laser Deposition and Atomic Layer Deposition enable the deposition of high density oxides on top of soft material such as organic and inorganic thin-films [30].

Finally, the realization of the BP-based photonic systems is also compatible with the deposition of BP by means of liquid exfoliation assisted by sonication [31]. This method is expected to be highly recommended in the case of photonic and optoelectronic applications given that uniform and large size of BP sheets can be obtained and easily deposited [32]: BP active layers with lateral dimensions of the order of tens of micrometers will avoid the use of localized microscopic optical probes to characterize the performance of BP-based PhC and microcavities.

Conclusion

We have suggested in this work the design of acBP and zzBP based 1D photonic crystals and microcavities, by simulations based on the transfer matrix method. Taking into account the findings reported in Ref. [12] we have considered the in-plane anisotropy of BP. In the 1D photonic crystals, BP is alternated with indium tin oxide layers, ensuring a charge transport along the refractive index modulation (i.e. normal to the layer planes). Instead, in the microcavity a trilayer SiO₂/BP/SiO₂ a defect layer between two SiO₂/GeO₂ photonic crystals (usually called distributed Bragg reflectors, DBR) has been employed. A photonic band gap arising in the photonic crystals and a cavity mode in the microcavity are very promising for the fabrication of BP based photonic structures for applications as sensing and light management.

References

- [1] Tománek D 2015 Interfacing graphene and related 2D materials with the 3D world *J. Phys. Condens. Matter* **27** 133203
- [2] Houssa M, Dimoulas A and Molle A 2015 Silicene: a review of recent experimental and theoretical investigations *J. Phys. Condens. Matter* **27** 253002
- [3] Churchill H O H and Jarillo-Herrero P 2014 Two-dimensional crystals: Phosphorus joins the family *Nat. Nanotechnol.* **9** 330–1
- [4] Li L, Yu Y, Ye G J, Ge Q, Ou X, Wu H, Feng D, Chen X H and Zhang Y 2014 Black phosphorus field-effect transistors *Nat. Nanotechnol.* **9** 372–7

- [5] Liu H, Du Y, Deng Y and Ye P D 2015 Semiconducting black phosphorus: synthesis, transport properties and electronic applications *Chem Soc Rev* **44** 2732–43
- [6] Zhang S, Yang J, Xu R, Wang F, Li W, Ghufran M, Zhang Y-W, Yu Z, Zhang G, Qin Q and Lu Y 2014 Extraordinary Photoluminescence and Strong Temperature/Angle-Dependent Raman Responses in Few-Layer Phosphorene *ACS Nano* **8** 9590–6
- [7] Liu H, Neal A T, Zhu Z, Luo Z, Xu X, Tománek D and Ye P D 2014 Phosphorene: An Unexplored 2D Semiconductor with a High Hole Mobility *ACS Nano* **8** 4033–41
- [8] Buscema M, Groenendijk D J, Blanter S I, Steele G A, van der Zant H S J and Castellanos-Gomez A 2014 Fast and Broadband Photoresponse of Few-Layer Black Phosphorus Field-Effect Transistors *Nano Lett.* **14** 3347–52
- [9] Qiao J, Kong X, Hu Z-X, Yang F and Ji W 2014 High-mobility transport anisotropy and linear dichroism in few-layer black phosphorus *Nat. Commun.* **5**
- [10] Rodin A S, Carvalho A and Castro Neto A H 2014 Strain-Induced Gap Modification in Black Phosphorus *Phys. Rev. Lett.* **112**
- [11] Wang X, Jones A M, Seyler K L, Tran V, Jia Y, Zhao H, Wang H, Yang L, Xu X and Xia F 2015 Highly anisotropic and robust excitons in monolayer black phosphorus *Nat. Nanotechnol.* **10** 517–21
- [12] Mao N, Tang J, Xie L, Wu J, Han B, Lin J, Deng S, Ji W, Xu H, Liu K, Tong L and Zhang J 2016 Optical Anisotropy of Black Phosphorus in the Visible Regime *J. Am. Chem. Soc.* **138** 300–5
- [13] Yablonovitch E 1987 Inhibited Spontaneous Emission in Solid-State Physics and Electronics *Phys. Rev. Lett.* **58** 2059–62
- [14] John S 1987 Strong localization of photons in certain disordered dielectric superlattices *Phys. Rev. Lett.* **58** 2486–9
- [15] Criante L and Scotognella F 2012 Low-Voltage Tuning in a Nanoparticle/Liquid Crystal Photonic Structure *J. Phys. Chem. C* **116** 21572–6
- [16] Passoni L, Criante L, Fumagalli F, Scotognella F, Lanzani G and Di Fonzo F 2014 Self-Assembled Hierarchical Nanostructures for High-Efficiency Porous Photonic Crystals *ACS Nano* **8** 12167–74
- [17] Liu X, Galfsky T, Sun Z, Xia F, Lin E, Lee Y-H, Kéna-Cohen S and Menon V M 2014 Strong light–matter coupling in two-dimensional atomic crystals *Nat. Photonics* **9** 30–4
- [18] Figueroa del Valle D G, Aluicio-Sarduy E and Scotognella F 2015 Photonic band gap in 1D multilayers made by alternating SiO₂ or PMMA with MoS₂ or WS₂ monolayers *Opt. Mater.* **48** 267–70
- [19] König T A F, Ledin P A, Kerszulis J, Mahmoud M A, El-Sayed M A, Reynolds J R and Tsukruk V V 2014 Electrically Tunable Plasmonic Behavior of Nanocube–Polymer Nanomaterials Induced by a Redox-Active Electrochromic Polymer *ACS Nano* **8** 6182–92

- [20] Malitson I H 1965 Interspecimen Comparison of the Refractive Index of Fused Silica *J. Opt. Soc. Am.* **55** 1205–8
- [21] Fleming J W 1984 Dispersion in GeO₂-SiO₂ glasses *Appl. Opt.* **23** 4486
- [22] Born M and Wolf E 2000 *Principles of Optics: Electromagnetic Theory of Propagation, Interference and Diffraction of Light* (CUP Archive)
- [23] Bellingeri M, Kriegel I and Scotognella F 2015 One dimensional disordered photonic structures characterized by uniform distributions of clusters *Opt. Mater.* **39** 235–8
- [24] A. Chiasera, F. Scotognella, L. Criante, S. Varas, G. Della Valle, R. Ramponi and M. Ferrari 2015 Disorder in Photonic Structures induced by random layer thickness *Sci. Adv. Mater.* **7** 1207–12
- [25] Xiao X, Wenjun W, Shuhong L, Wanquan Z, Dong Z, Qianqian D, Xuexi G and Bingyuan Z 2016 Investigation of defect modes with Al₂O₃ and TiO₂ in one-dimensional photonic crystals *Opt. - Int. J. Light Electron Opt.* **127** 135–8
- [26] Jeon P J, Lee Y T, Lim J Y, Kim J S, Hwang D K and Im S 2016 Black Phosphorus–Zinc Oxide Nanomaterial Heterojunction for p–n Diode and Junction Field-Effect Transistor *Nano Lett.* **16** 1293–8
- [27] Lin S, Liu S, Yang Z, Li Y, Ng T W, Xu Z, Bao Q, Hao J, Lee C-S, Surya C, Yan F and Lau S P 2016 Solution-Processable Ultrathin Black Phosphorus as an Effective Electron Transport Layer in Organic Photovoltaics *Adv. Funct. Mater.* **26** 864–71
- [28] Kim J S, Jeon P J, Lee J, Choi K, Lee H S, Cho Y, Lee Y T, Hwang D K and Im S 2015 Dual Gate Black Phosphorus Field Effect Transistors on Glass for NOR Logic and Organic Light Emitting Diode Switching *Nano Lett.* **15** 5778–83
- [29] Avsar A, Vera-Marun I J, Tan J Y, Watanabe K, Taniguchi T, Castro Neto A H and Özyilmaz B 2015 Air-Stable Transport in Graphene-Contacted, Fully Encapsulated Ultrathin Black Phosphorus-Based Field-Effect Transistors *ACS Nano* **9** 4138–45
- [30] Natali D, Chen J, Maddalena F, García Ferré F, Di Fonzo F and Caironi M 2016 Injection Length in Staggered Organic Thin Film Transistors: Assessment and Implications for Device Downscaling *Adv. Electron. Mater.* 1600097
- [31] Serrano-Ruiz M, Caporali M, Ienco A, Piazza V, Heun S and Peruzzini M 2016 The Role of Water in the Preparation and Stabilization of High-Quality Phosphorene Flakes *Adv. Mater. Interfaces* **3** 1500441
- [32] Xu J-Y, Gao L-F, Hu C-X, Zhu Z-Y, Zhao M, Wang Q and Zhang H-L 2016 Preparation of large size, few-layer black phosphorus nanosheets via phytic acid-assisted liquid exfoliation *Chem Commun* **52** 8107–10